The Nucleation and Solidification of Al-Ti Alloys

J. CISSÉ, H. W. KERR, AND G. F. BOLLING

A series of hyperperitectic Al-Ti alloys at 0.35, 0.5, 0.7 and 0.8 wt pct Ti has been frozen at rates varying from less than 1°C/s to in excess of 100°C/s. Cooling-curve analyses, metallographic and microprobe examinations, taken altogether, allow identification both of the nucleants and the solidification modes acting in this important alloy system. Two sets of conclusions are drawn, one in general about low concentration peritectic systems like Al-Ti, and the other about particular interactions in Al-Ti. For example, it is revealed that Al_xTi compounds exist; Al_3Ti, Al_xTi and Al are nucleated by TiC; and Al_xTi and TiC are both nucleants for aluminum.

THE nucleation of solid and solidification in aluminum-titanium alloys have been studied for many years. The reasons for this are obvious. At low concentrations, Ti provides an inoculant for aluminum leading to a pronounced grain refinement. The existence of the peritectic point may provide the reaction for the inoculating nucleus by forming Al_3Ti. On the other hand, carbon which is a common minor impurity in Al may provide the inoculating nucleus, as TiC. In fact, we recently showed that nucleation by both these agents can be valid, thus supporting many other individual observations and arguments.[1]

The study of this sytem has now proceeded much further. Here we shall report new facts, both about nucleation and about solidification; for we have fonnd that the two are not readily separated.

After describing our experimental techniques, we begin the results with microprobe analyses of dendrites. These show significant supersaturation of Ti in Al, so that initial solidification occurred far from equilibrium. In fact, the phase diagram is a dangerous guide to the possible events which might occur over wide freezing rates or at different concentrations.

Our later steps involve

a) systematic observations about cooling rates and freezing temperatures;

b) changing amounts of second phase at different cooling rates;

c) changing growth forms and grain sizes at different cooling rates;

d) identifications of new Al_xTi compounds;

e) fine microprobe analyses of the carbon-rich nuclei associated with Al and with Al_xTi compounds (nucleants);

f) combinations of the above measurements.

Most of this detailed investigation is restricted to alloys above 0.15 wt pct Ti. At all freezing rates solidification of alloys with less titanium cannot encounter the peritectic reaction. Hence we call alloys at lower concentrations hypoperitectic and the alloys we deal with, above 0.15 wt pct, hyperperitectic. Since we have investigated nucleation and grain size in the hypoperitectics, attributing grain refinement to the action of TiC in our system,[1] there seems to be no mystery for these alloys.

A brief summary is given at the end of the paper. We argue that nearly all the observations made to date in the Al-Ti system can be understood in the light of the results presented here.

I. EXPERIMENTAL TECHNIQUES

Specimens of various titanium concentrations, made up from aluminum of 99.99 pct purity and a commercial titanium "hardener" were melted and cast from 100°C above the liquidus temperature, usually into a cylindrical graphite mold of 2 cm radius. The temperatures close to the bottom of each specimen were monitored using a fine chromel-alumel thermocouple, which projected 2 mm up from the bottom of the mold with its tip covered by a thin layer of alumina cement. A high speed (up to 2 cm/s chart speed) recorder, with one or two millivolts full scale, was employed. The overall cooling rates were varied by preheating the mold, allowing still air cooling starting with a room-temperature mold, or cooling the mold during and after casting with a water or air spray. The rate of cooling was not constant, and we have chosen to measure it from the tangent as close as possible to, and above, an inflection point.

Microsections of regions very close to the thermocouple tip were made by various techniques for optical microscopy.

Counts of 60 to 100 s were made with a three spectrometer ARL-EMX electron microprobe on points of interest, and the raw data analyzed by the Multi 8, Magic 4, or Ford programs[2] for absorption, fluorescence and atomic number corrections. These programs differ in their handling of the atomic number corrections, but there remains considerable controversy about which program is most correct.[2] We have chosen to average the results of three programs in giving our results.

II. RAPID FREEZING: Ti SUPERSATURATION AND DISTRIBUTION

Rapid freezing leads to dendritic growth. These very rapid freezing experiments occurred too quickly to give meaningful inflection points on the cooling curves, but from the time for complete liquid to solid transformation (approximately 20 s) we estimate the velocities of the dendrite tips to be between 0.1 and 1 cm/s. Titanium profiles obtained with the electron microprobe are

J. CISSÉ, formerly of the Ford Scientific Staff, is now Senior Engineer, Société National d'Etude et de Construction de Moteurs d'Aviation, Gennevilliers, France. H. W. KERR, is Associate Professor, Department of Mechanical Engineering, University of Waterloo, Waterloo, Ontario, Canada. G. F. BOLLING is associated with Product Planning and Research, Ford Motor Co., 20,000 Rotunda Dr., Dearborn, Mich. 48121.

Manuscript submitted May 21, 1973.

shown in Fig. 1. The effective resolution was 4 microns. This can be supported by noting that the finest profile at 0.5 wt pct Ti was obtained across a dendrite optically found to be 11 microns wide. The microprobe concentration profile is 15 microns in width. Another traverse in a 0.35 wt pct Ti specimen was taken across a dendrite of approximately 30 microns optical width. The microprobe concentration profile is 37 microns wide. Two features of these profiles are of interest; the initial concentration transients, and the maximum concentration reached. For the system that freezes with a purer solid ($k_0 < 1$) many studies[3-5] have shown that the solute composition at dendrite centers can drop far below the average composition. This large sudden change can be easily explained. The case of $k_0 < 1$ requires only an efflux over the occupied volume of the dendrite tip, so that even for very fast velocities the predicted[6] centerline compositions can be achieved. For the system with $k_0 > 1$, the simple opposite of this will not hold. In order to obtain sufficient solute for the centerline to reach its expected solute level, an influx must be obtained from the liquid over a volume approximately k_0 times the dendrite tip radius. When the dendrite velocity is very large, as in the present experiments, this required influx will result in an initial transient.

In support of this reasoning, a relative depletion of titanium is observed in the centers of several overall titanium-rich dendrites. Even across the profiles at low Ti (0.06 wt pct), where the level is initially so low that the sectioning problem will be worst, one of the two profiles does definitely indicate a hill-with-valley profile. It is probably significant that this profile is narrower than the other in the same alloy, indicating that the section was closer to the dendrite centerline. Across profiles at high Ti (0.5 wt pct), the dendrites were themselves too narrow to allow the centerline depletion, if any, to be resolved. At the intermediate concentration of 0.35 wt pct Ti, both the profiles shown exhibit the hill-with-valley concentrations in good agreement with the simple description. If we reasonably assume that the liquid at the interface essentially remains at the concentration C_0 after the small amount of initial solidification, we can suppose that the maximum concentration reached in the solid dendrite is k_0 Co. Since this implies local liquid-solid equilibrium, these liquid and solid compositions can be plotted on the equilibrium or extended liquidus and solidus lines between liquid and α-Al, as shown in Fig. 2. The possible errors could lead to a result too low in solute concentration if there were diffusion in the solid (doubtful in our experiments because the specimens were at room temperature in about one minute), or if the sectioning was poor as already mentioned.

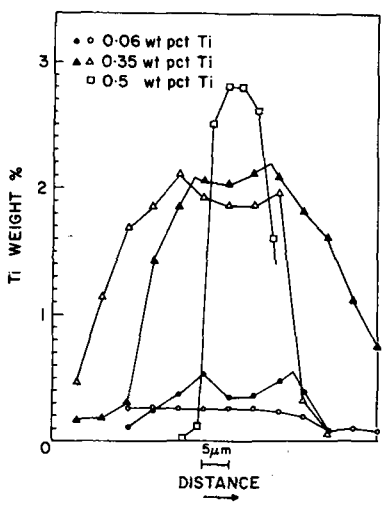

Fig. 1—Microprobe analyses through primary dendrite stalks in different Al-Ti alloys.

Comparison of Figs. 1 and 2 with the established phase diagram shows that the maximum titanium concentrations are supersaturated solid solutions. Although supersaturated solutions have been observed in other systems, the previous lack of concurrent thermal analysis masked an important consequence; these supersaturated solutions solidified above the peritectic reaction temperature.

III. COOLING RATES AND FREEZING TEMPERATURES

3.1 In establishing Fig. 2 we used freezing rates faster than any we shall describe for more controlled, and hence measurable, cooling. In these recorded cooling experiments we have frozen "pure" Al, and Al-Ti alloys containing 0.35, 0.5, 0.7 and 0.8 wt pct Ti. We shall limit most of our report to the alloys at 0.35 wt pct Ti and 0.8 wt pct Ti, since these results illustrate all of the observed effects.

In Fig. 3 we present the results for Al. It can be

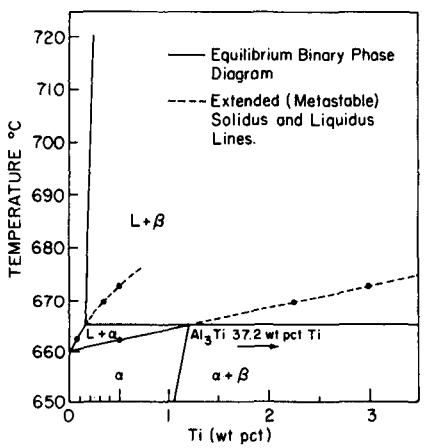

Fig. 2—Equilibrium and metastable phase diagram for the Al-Ti system, as constructed from Fig. 1.

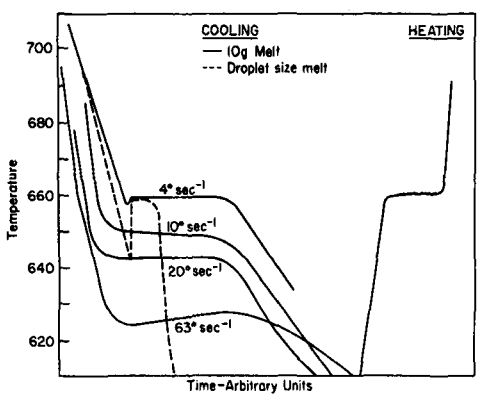

Fig. 3—Cooling curves recorded for various cooling rates in pure aluminum. Increased cooling rates always decreased the observed plateaux temperatures.

seen that respectable plateaux are obtained up to 20°C/s. But above approximately 4°C/s the plateaux are below the freezing point at 660°C. This is very important. Since slow-cooled Al was used to calibrate thermocouples, the appearance of other effects to be reported above 660°C cannot be regarded as spurious thermal pickups. Results from a very small melt sample (droplet size) are included to show that recalescence and the plateau are a function of the arrangement. Finally, we see that 660°C is obtained without fail on melting.

3.2 Cooling curves for Al-0.35 wt pct Ti are reproduced at different scales in Fig. 4. At the two slower rates we see the peritectic temperature of 665°C appear as a primary event. At higher rates we find higher temperature responses—and the higher the rate, the higher the response temperatures. Because of the required size reduction, curves (5) and (6) cannot show the details of the responses at 20°C/s and at 48°C/s, but the high nucleation temperatures are evident from the reduced slope close to the indicated temperatures, followed by steeper slopes below approximately 660°C. The nucleation temperatures given by small inflection points are shown in the figure.

Similar observations were unquestionably found at 0.5, 0.7 and 0.8 wt pct Ti as well. It was also observed that the higher the Ti concentration, the more difficult to observe a plateau response at the higher rates (Table I). We reproduce the results for 0.8 wt pct Ti in Fig. 5 to illustrate the worst case. No real plateau was found at any cooling rate, and a tangent intersection had to be used to determine a response temperature. Steeper slopes, similar to those in Fig. 4, were found below 660°C at the slower cooling rates, but are off the diagrams. Some lower temperature reactions can be seen at the intermediate freezing rates; even these disappear at the highest rates.

The observed results summarized in Table I, with underlining distinguishing arrest temperatures (plateaux), are assembled in Fig. 6 to show the two reasonable trends; that there is an elevation of some observable reaction temperature at higher freezing rates, and that this elevation becomes higher the higher the Ti concentration. These trends are independent of the exact results obtained, that is, the exact temperature elevations.

At the least, the first result can be based only upon observed plateaux and cannot therefore be discarded as a transient. It thus may be concluded that either there cannot be a single reaction temperature, or there cannot be a unique "second" (properitectic)* phase composition, or both. We shall demonstrate shortly the second possibility; different properitectic phase compo-

*The term protoperitectic might also be used.

Table I. Cooling Arrests in Al-Ti Alloys
(Underlined Temperatures are Plateau Values)

Cooling Rate, °C/s	Composition Wt Pct Ti			
	0.35	0.5	0.7	0.8
<1	665	665	665	665
1	665		665	
1.2		666.75		
1.5		664.5	666.25	
3	665			669.25
3.5		667		
4	667		667.25	670.25
10		(674)		671.25
12.5			678	
16	668.5			
20	669.25			
41		?		
48	670			
66				?
76			?	?
86			?	?

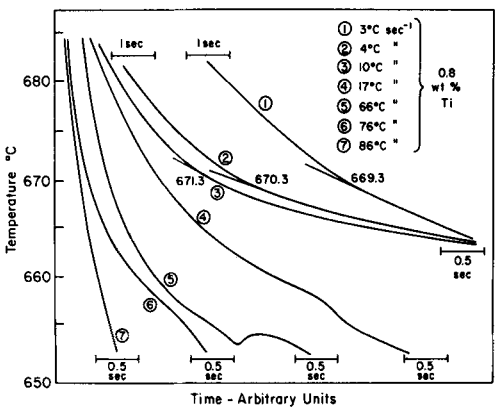

Fig. 5—Cooling curves recorded for various cooling rates in Al-0.8 wt pct Ti specimens. The tendency for increased nucleation temperatures with increased cooling rate was apparent only at lower rates.

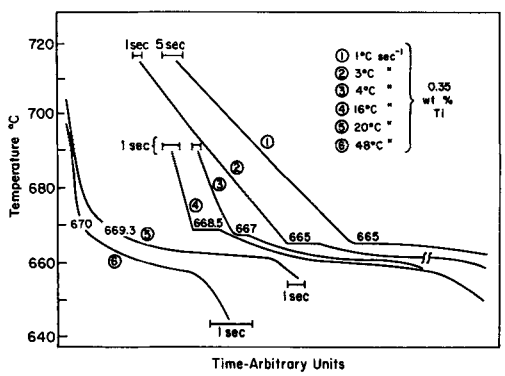

Fig. 4—Cooling curves recorded for various cooling rates in Al-0.35 wt pct Ti specimens. Increased cooling rates increased the observed plateaux temperatures.

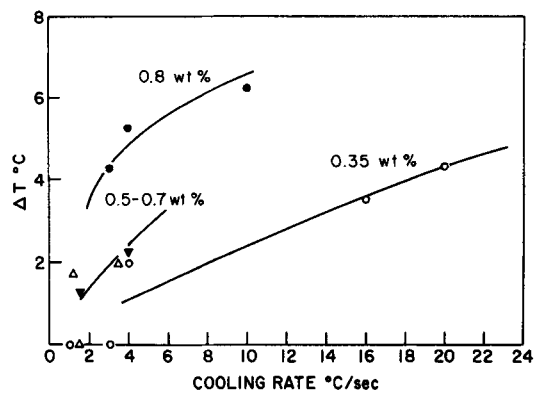

Fig. 6—The summary of the correlation between increased cooling rates and increased nucleation temperatures for different Al-Ti alloys.

sitions. But it is first worthwhile to comment on the more obvious variations in amount and form of the "second" phases(s).

IV. CHANGING AMOUNTS OF SECOND PHASE

Metallographic results are shown in Figs. 7 and 8 for the two reference alloys 0.35 wt pct Ti and 0.8 wt pct Ti (reference cooling curves in Figs. 4 and 5). It can readily be seen in Fig. 7 that the amount of properitectic phase decreases with increasing cooling rate. The results obtained by Quantimet Analysis are given in Table II. Care was taken to distinguish second phase from porosity as indicated.

Only two representative fields are shown in Fig. 8 as related to the results of Table II. Much higher cooling rates had to be reached in order to eliminate a properitectic phase at this higher concentration level. At 500°C/s an apparent single phase could be achieved in small specimens. For some reason little porosity was observed in these alloys.

V. CHANGING GROWTH FORMS AND GRAIN SIZES

In addition to changes in the quantity of second phase, Figs. 7 and 8 show that the forms of the second phase change with cooling rate for any composition. At slow cooling rates smooth regular plate-like particles, some of which show the butterfly shape typical of twin-plane re-entrant edge (TPRE) growth[7] are seen along with closed-end form particles (Figs. 7 and 9). Unfortunately our etches do not allow us to determine if the closed-end form particles also contain twins. At very slow rates, with higher titanium concentrations, the growth forms again indicate TPRE growth but the surfaces are less smooth because of the subsequent peritectic reaction (Fig. 10). We should remark that in a very slowly cooled alloy Al nucleation frequency can vary throughout an ingot. Where the Al_3Ti settles there is a grain size somewhat related to the Al_3Ti, but less than in a one-to-one ratio. At the ingot top there is an even coarser grain size, being without Al_3Ti and more dendritic.

Increased growth rates decrease the aspect ratio of the second phase particles, making them irregular bodies with incomplete surfaces (Figs. 7 and 11), with no evidence of TPRE growth. This apparent reduction in the importance of TPRE growth with increased growth ratio is consistent with the observation of Faust and John[7] in other compounds.

During this progression the grain size of a given alloy decreases continually while a second phase is visible, as may be seen by comparing Figs. 9, 11, and 12. This may be due to an increased density of nucleating particles at faster cooling rates, but it seems impossible to metallographically determine the distribution of such particles. Alternatively it may be associated with altered compositions or crystal structures at nucleant surfaces. Although we will show shortly that the composition of the intermetallic phase does change with cooling rate, we have no direct evidence about the nucleant surfaces.

Without observable intermetallic particles the grain size becomes larger. Nucleation then appears to be due to black spots (Fig. 13).

VI. NEW Al_xTi COMPOUNDS

In order to further investigate the non-equilibrium possibilities in the Al-Ti system, microprobe analysis of intermetallic particles was undertaken. After preliminary work it was decided to investigate most closely the more plentiful particles in the Al-0.8 wt pct Ti alloy.

Measurements were made under 10, 15 and 20 KV. As expected, there was a shift toward higher Al values (lower Ti values) at the increased voltages. At 10 KV the beam penetrates ~1.2 μ in Al and the X-ray resolution diameter ~2.2 μ. At 20 KV these values increase respectively to ~4.5 μ and ~5.5 μ. We must expect that part of the matrix was included at a 20 KV examination of the second phase particles shown in Fig. 8 (~100°C/s). This higher penetration test was done intentionally to estimate and avoid a "depth of penetration" criticism for pick up of background Al at 10 KV.

Results are shown in Fig. 14 as amassed for two undifferentiated cooling rates ($\ll$100°C/s and ~100°C/s) in order to show the penetration trend. Obviously at 20 KV, there is a background Al pick up in the microprobe results. It is important to note that there is, even so, a distinct separation into an upper Ti and a lower Ti concentration range. This separation appearing at 20 KV and 10 KV is therefore independent of background or lateral pick up.

The results for 10 KV alone, calculable to be free from matrix pickup, are grouped in Fig. 15. A slightly different interval is chosen for the display histograms and there is a differentiation into the two cooling rate sets. We see that,

i) Al_3Ti does exist.

ii) Non-equilibrium Al_xTi compounds must exist (not necessarily at the compositions shown).

iii) A spectrum of Al_xTi or at least two definite new compounds exist.

iv) There is more non-equilibrium Al_xTi, the higher the cooling rate.

The amount of Al_xTi as it existed in dispersion was not sufficient for X-ray identifications, and we did not successfully conclude electron microscope work. We cannot therefore comment if there are graded compounds, distinct compounds, new crystal structures, and so forth.

We suspect, however, that volume fractions of the Al_xTi's compared to the fraction of Al_3Ti are much higher than those shown, especially for rates $\geq$100°C/s. Only large particles could be analyzed without forcing an Al background pick up. These large particles were far outnumbered by many smaller particles.

Finally, we remark that measurements were also made in Al-0.35 wt pct Ti. These are sufficient to assure us that the same three compound groupings existed in this lower concentration alloy.

VII. FINE MICROPROBE ANALYSIS OF "BLACK SPOT" NUCLEI

A careful search was made for the larger, but representative, "black spots" that were usually found to

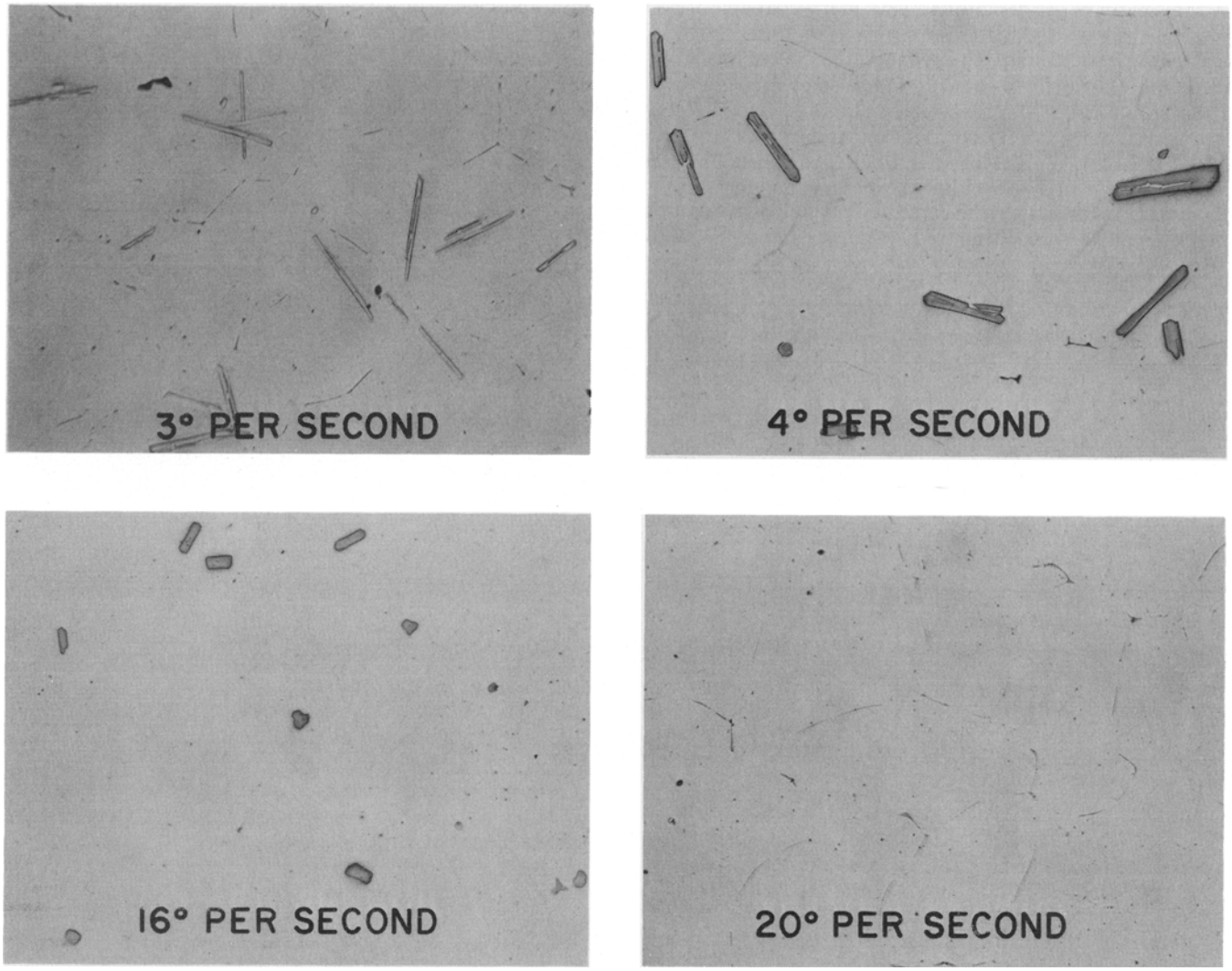

Fig. 7—Typical microstructures in Al-0.35 wt pct Ti specimens cooled at different rates. Magnification 150 times.

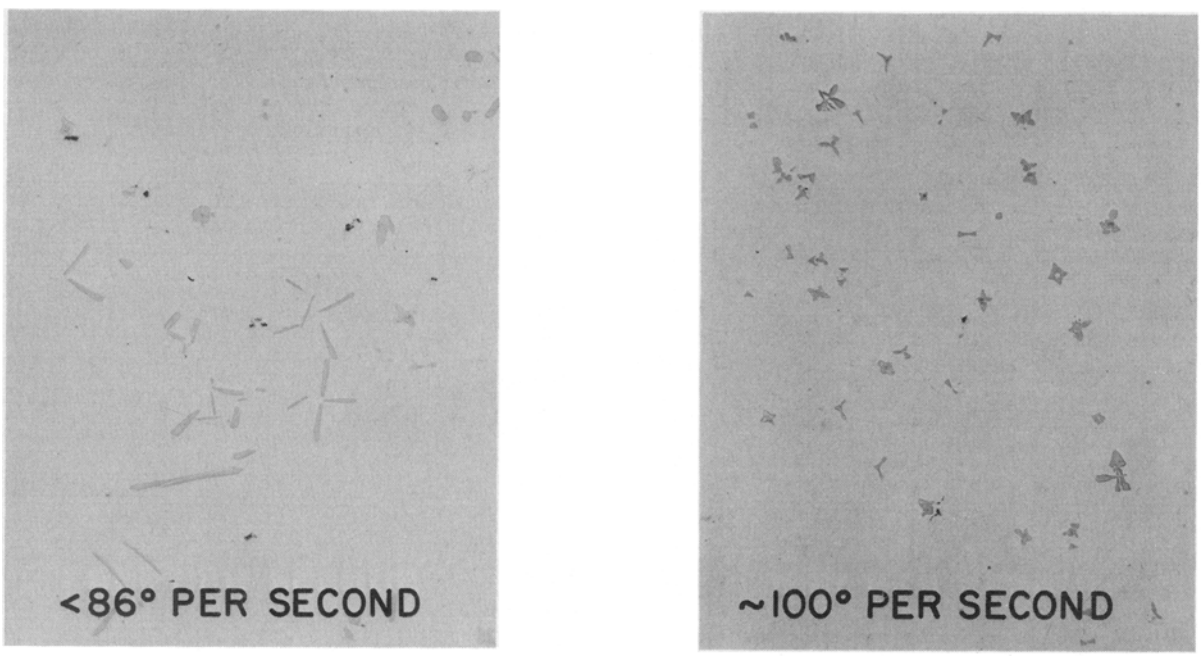

Fig. 8—Typical microstructures in Al-0.8 wt pct Ti specimens cooled at two different rates. Magnification 150 times.

be the origin of Al dendrites. One metallographic example is shown in Fig. 16(*a*), along with X-ray back scattering results and a representative scanning microscope view of this particle (Fig. 16(*b*) through (*d*). If the sum total of the three spectrometer microprobe analysis of Al + C + Ti departed more than 10 pct from a 100 pct total, the result was discarded. Fig. 17 gives the end result of five readings, which are relatively consistent. For this alloy (0.35 wt pct Ti) the black spot cannot be reconciled to Al_3Ti and can be concluded to be the result of a compound in a situation like: TiC with an Al background (the black spot is small); Ti_xAl C, or some Ti-Al-C compound with an Al background.*

*TiC was also observed by electron diffraction on residues obtained by specific dissolution of the Al matrix. Such indirect results are strong support for nucleation by this compound

Table II. Amount of Second Phase vs Cooling Rate

Alloy, wt pct	Cooling Rate, °C s^{-1}	2nd Phase, pct	Porosity, pct
Al-0.35Ti	3	1	0.24
	4	0.57	0.13
	16	0.38	0.05
	20	0.0	0.0
Al-0.8Ti	<86	1.6	0.0
	86	1.0	0.0
	~100	0.96	0.0
	~500	0.0	0.0

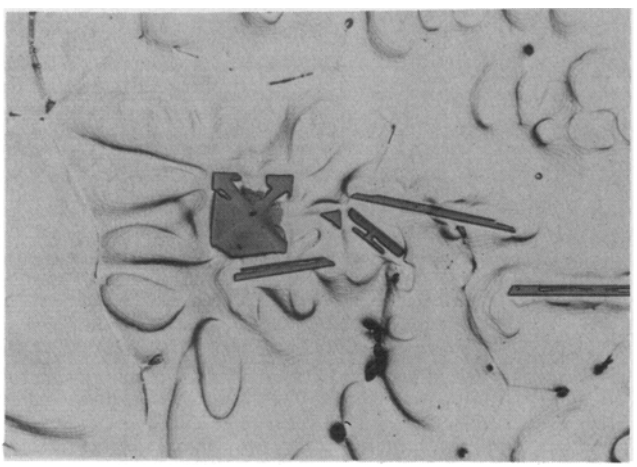

Fig. 9—Closed end form and smooth regular intermetallic particles in Al-0.35 wt pct Ti alloy cooled at 3°C/sec. Magnification 200 times.

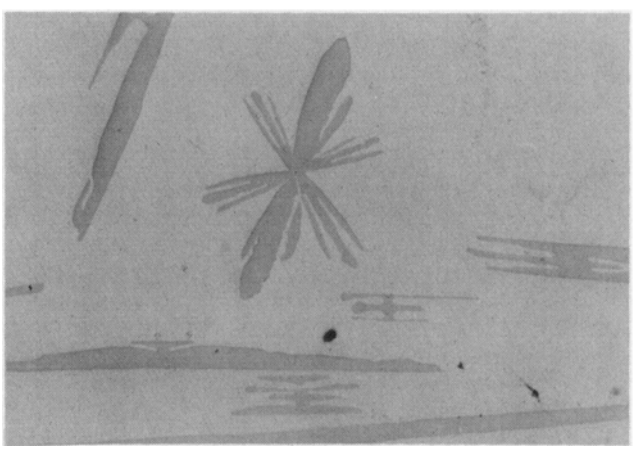

Fig. 10. Developed but irregular intermetallic particles in Al-0.8 wt pct Ti alloy cooled at a very slow rate. Magnification 150 times.

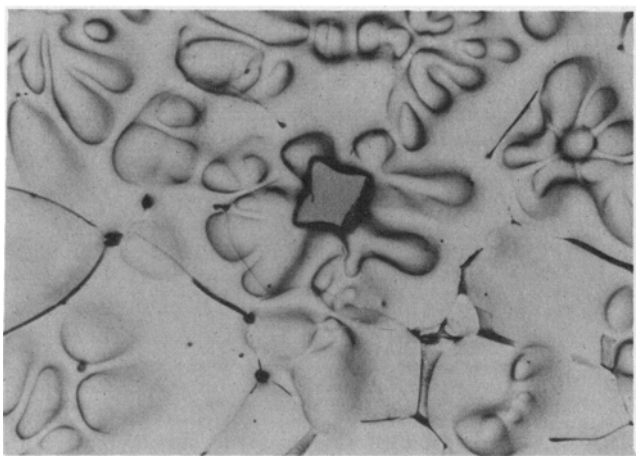

Fig. 11—Irregular intermetallic particle in Al-0.35 Ti alloy cooled at 4°C/sec. Magnification 200 times.

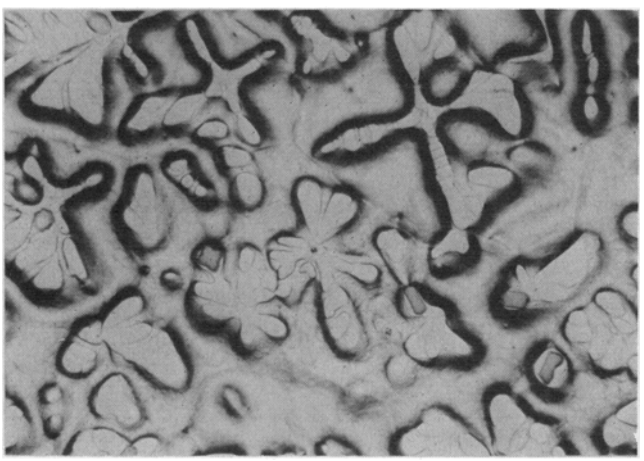

Fig. 12—Irregular intermetallic particles, and at least one "black spot" nucleant in Al-0.35 wt pct Ti alloy cooled at a fast rate (16°C/s). Magnification 200 times.

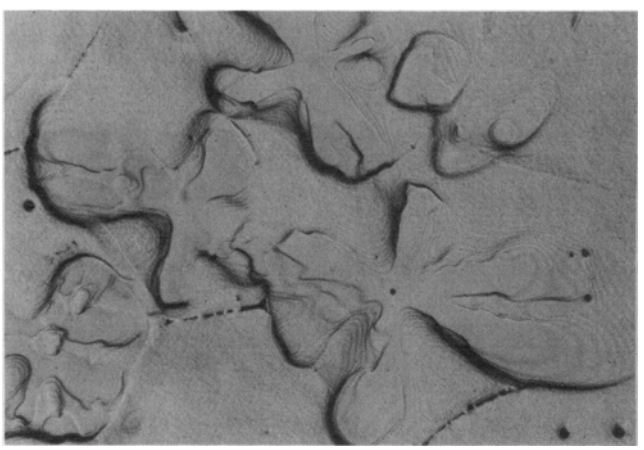

Fig. 13—"Black spot" nucleant in Al-0.35 wt pct Ti alloy cooled at a very fast rate (20°C/s). Magnification 200 times.

The higher concentration reference alloy Al-0.8 wt pct Ti was then found to contain Al_xTi that contained black spots themselves in their centers, as shown in Fig. 18. These were similarly analyzed to reveal the other result in Fig. 17. For this alloy, no matter what the Al_xTi composition we can assume from Fig. 15, the black spot cannot be reconciled to an Al_xTi but must again be one of the following combinations; TiC with a background near Al_3Ti (or an Al_xTi); or some other Ti-Al-C compound with an Al_3Ti (or an Al_xTi) background.

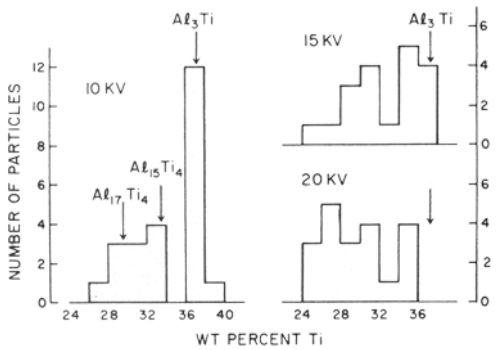

Fig. 14—Microprobe analyses of various nucleant particles in – 0.8 wt pct Ti specimens, including the effects of accelerating voltages used in the analyses.

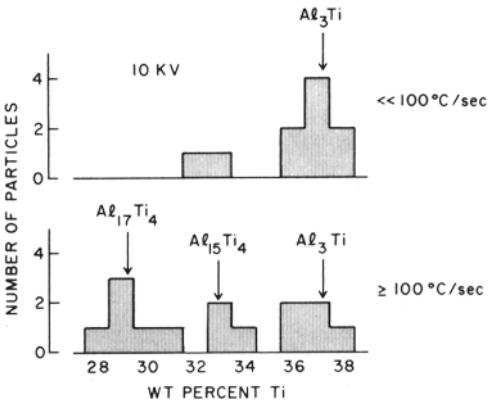

Fig. 15—Microprobe analysis of various nucleant particles in Al-0.8 wt pct Ti specimens cooled at two different rates. The accelerating voltage was low enough to prevent matrix excitation.

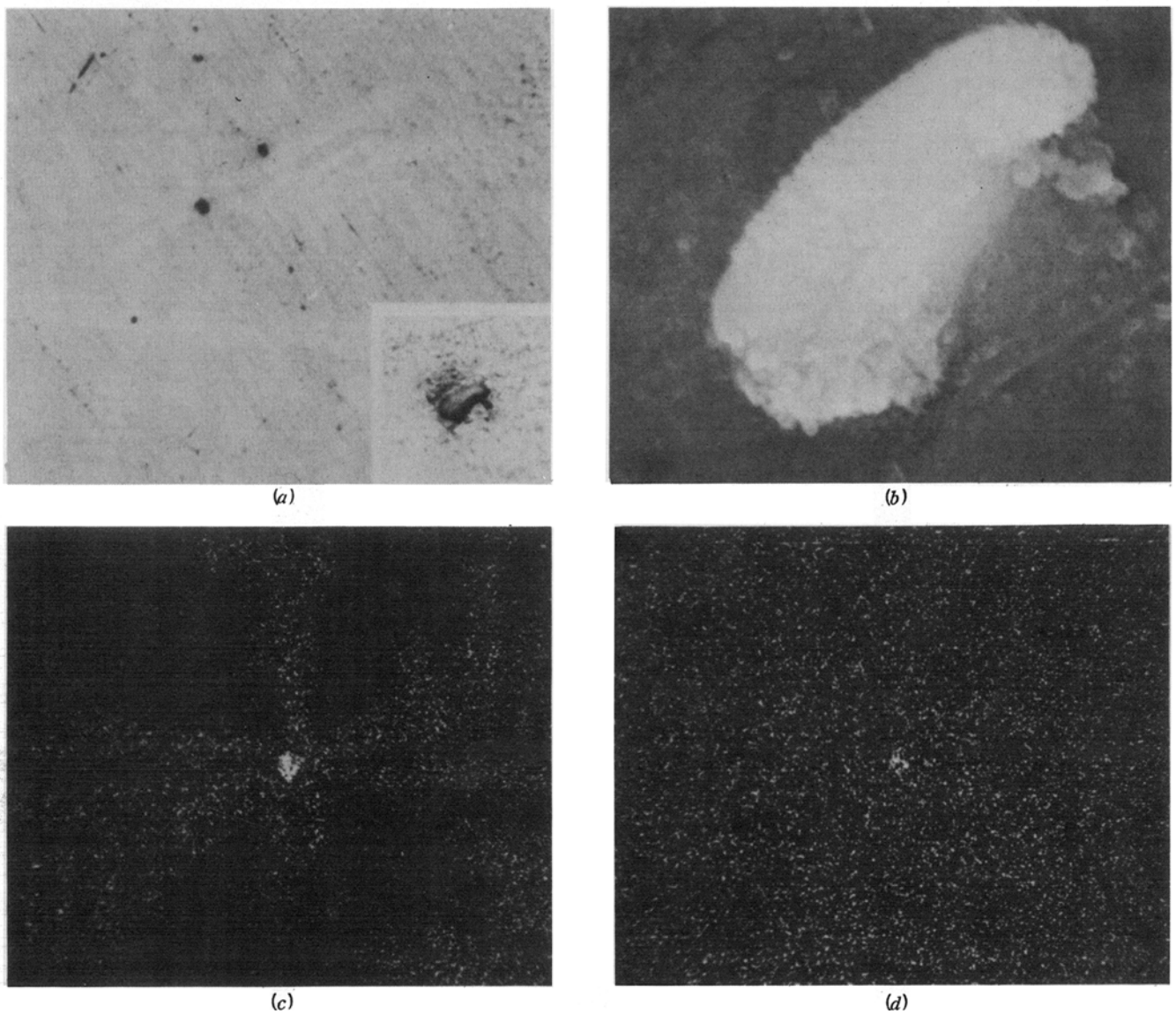

Fig. 16—(*a*) Optical (X200 and X1000), (*b*) scanning (X8000) and microprobe X-ray images for (*c*) titanium (10 kv X700) and (*d*) carbon (10 kv, X700) of a region including a "black spot" nucleant within an aluminum dendrite.

The microprobe background pick up is very important here because of the small black spot size. We conclude that it is very difficult to accept the idea of some supposed but unknown Al-Ti-C compound leading to an Al_xTi or to Al_3Ti. We strongly lean to the proven nucleating agent near the TiC composition. (This was suggested earlier by Delamore and Smith.)[8]

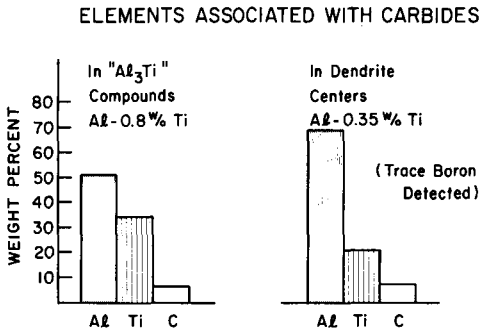

Fig. 17—Microprobe analyses of regions including "black spot" nucleants in Al_3Ti and in Al dendrites.

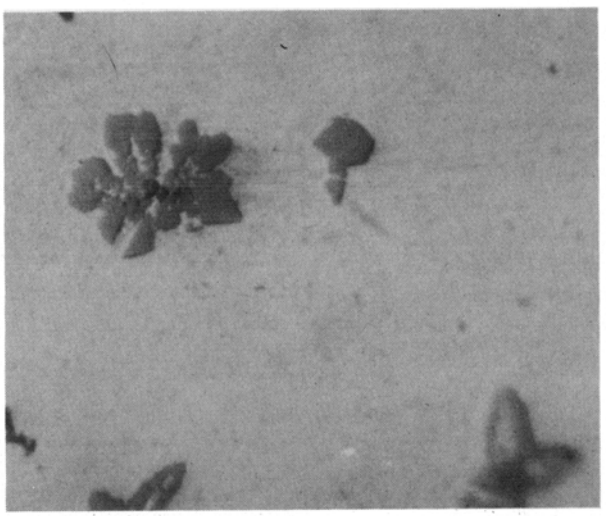

(a)

(b)

Fig. 18—(*a*) Optical (X1500), (*b*) scanning (X8000), and microprobe X-ray images using 10 kv (X1000) for (*c*) titanium (*d*) carbon (*e*) aluminum for regions including "black spot" nucleants within intermetallic compounds. (*b*) is of a different region from the other images.

VIII. COMBINATION OF THE MEASUREMENTS

Table III is a summary of the observations made for the Al-0.35 wt pct Ti alloy. It is indeed a summary of behavior in the whole system. With a few transpositions in cooling rates, the relative statements of Table III will apply to the Al-0.8 wt pct Ti alloy or to any of the others in the range 0.35 to 0.8 wt pct Ti.

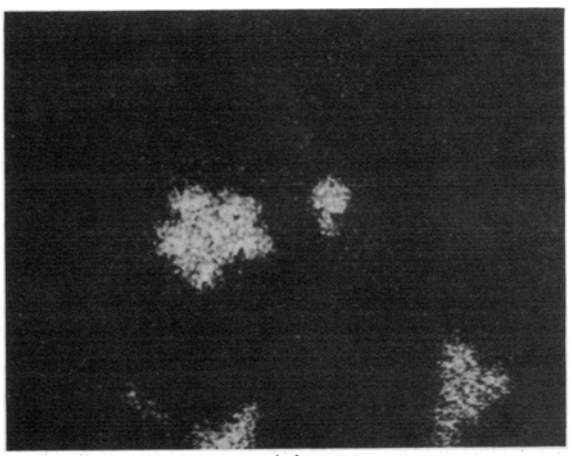

(c)

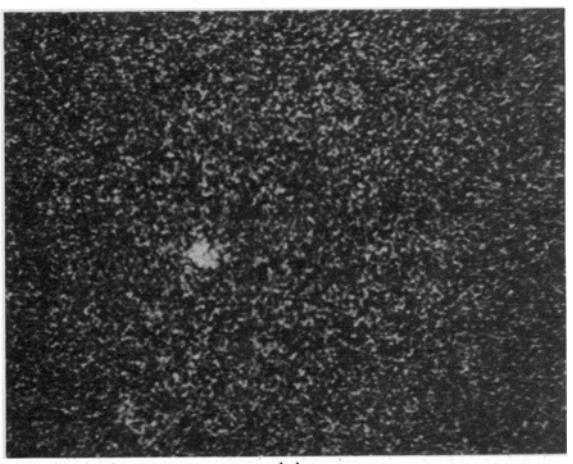

(d)

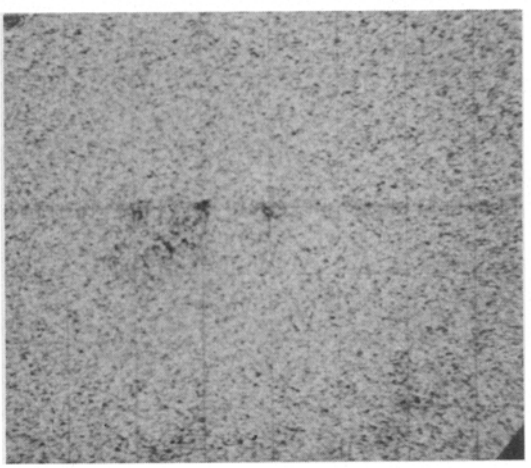

(e)

Table III. Summary Observations for Al-0.35 Wt Pct Ti

Cooling Rate, °C/s	ΔT, °C	Relative Grain Size	AlxTi		Nucleant
			Pct	Shape	
0.16	0	Large	Distributed by settling	Jagged, Irregular, Developed	TiC Al_3Ti
1	0	Large	(———— not measured ————)		
3	0	Moderate	1	Smooth, Regular	AlxTi (TiC)
4	2	Moderate	0.57	Smooth, Regular	AlxTi TiC
16	3.5	Small	0.38	Smooth, Irregular	TiC (AlxTi)
20	(4.3)	Large	0.0	None	TiC
48	(5)	Large	0.0	None	TiC

We have not stressed the observation of what is the apparent nucleant under a given set of conditions. We do so now in Table III. At the slowest rates any nucleant seems to serve; and we have positively identified Al_3Ti and TiC. The latter probably is responsible at melt surfaces because of settling effects of Al_3Ti. At higher rates the Al_xTi phase(s) can operate. Here we cannot exclude Al_3Ti, but neither has Al_3Ti been solely identified as a nucleant. At extreme rates TiC dominates and eventually must act alone, as evidenced by the important grain size inversion (about 20°C/s). This inversion, as we have previously noted,[1] may be related to the "complete" epitaxial relationship for Al on TiC only allowing one Al grain on each TiC particle, whereas the partial epitaxial relationship of Al on Al_3Ti, and probably on other Al_xTi phases, may allow several grains of Al on each intermetallic nucleant particle. Hence the initial high solute region in α-Al is continuous around carbide nucleants (Fig. 13), but may be discontinuous around an intermetallic particle, having nucleated different grains on different regions of the nucleant surface (Fig. 11 and Ref. 1).

It is clear that in an absolutely pure Al-Ti system, nucleation via TiC could not take place. Carbon is a common impurity; even 99.99 pct aluminum contains a few ppm, so that it is almost impossible to avoid this element. Moreover, in the short time of solidification no interaction between the specimens and crucible was evident, and the specimens easily slid out when solid.

Consequently, we believe our results to be representative, and useful in explaining industrial and other experimenters' results.

It can almost be said in answer to the long standing controversy[8-10] about the Al-Ti system that all previous answers (to: what is the nucleant?) are correct as long as the proper conditions are delineated.

IX. SUMMARY

We have presented a wide ranging set of experiments and results in the low concentration range of Al-Ti alloys. Some of these are relevant to peritectic transformations in general.[11] For a summary here we nevertheless recognize two classes of observation:

a) General conclusion for Peritectic Systems that preferentially incorporate solute ($k_0 > 1$):

i) Rapid growth occurs with solute-enriched dendrites. The microsegregation across the needle stalk of these dendrites will have a concentration inversion (Fig. 1), but it is not always measureable.

ii) The faster the freezing rate, the higher the temperature at which a peritectic type phase can occur. This is explained elsewhere.

iii) The faster the freezing rate, the less the amount of properitectic ("second") phase.

iv) The faster the freezing rate, the more incomplete the second phase growth form, at least partially because the second phase may be of changing composition.

b) Particular conclusion for Al-Ti alloys.

i) Non-equilibrium Al_xTi compounds exist. These vary in form and composition, depending on the freezing rate.

ii) Aluminum is nucleated by Al_xTi, and TiC.[1] Although Al_3Ti does exist, there is no proof that its external surfaces present a stoichiometric compound. We can only conclude that Al_xTi is a nucleant; Al_3Ti may be nucleant. Not all particles of Al_xTi act as nucleants.[1]

iii) Al_xTi is nucleated by a compound complex of (Al, Ti, C), or more probably, by TiC.

iv) Under extremely fast freezing in alloys, where Al_3Ti might be a nucleant for equilibrium conditions, only TiC or the (Al, Ti, C) complex is a nucleant. See the grain size inversion given in Table III.

v) For hypoperitectic alloys (< 0.15 wt pct Ti) TiC is the only active nucleant in our experiments.[1]

vi) At very slow freezing rates there can be a spatial separation between Al_3Ti and the other possible nucleant.

A consideration of Table III can be used to explain nearly all observations of nucleation of Al-Ti alloys.

ACKNOWLEDGMENTS

The microprobe analysis was carried out with the very capable guidance of Mr. J. Tabock. Part of this work was supported by a grant from the National Research Council of Canada.

REFERENCES

1. J. Cissé, G. F. Bolling, and H. W. Kerr: *J. Cryst. Growth,* 1972, vol. 13/14, pp. 777-81.
2. J. Tabock: Ford Motor Co., private communication.
3. M. C. Flemings, D. R. Poirier, R. V. Barone, and H. D. Brody: *J. Iron Steel Inst.,* 1970, vol. 208, p. 371.
4. F. Weinberg and E. Teghtsoonian: *Met. Trans.,* 1972, vol. 3, pp. 93-111.
5. T. F. Bower, H. D. Brody, and M. C. Flemings: *Trans. TMS-AIME,* 1966, vol. 236, pp. 624-34.
6. G. F. Bolling and W. A. Tiller: *J. Appl. Phys.,* 1961, vol. 32, pp. 2587-605.
7. J. W. Faust and H. F. John: *J. Phys. Chem. Solids,* 1964, vol. 25, p. 1407.
8. G. W. Delamore and R. W. Smith: *Met. Trans.,* 1971, vol. 2, pp. 1733-38.
9. A. Cibula: *J. Inst. Metals,* 1949, vol. 76, pp. 321-60.
10. F. A. Crossley and L. F. Mondolfo: *Trans. AIME,* 1951, vol. 191, pp. 1143-48.
11. H. W. Kerr, J. Cissé, and G. F. Bolling: accepted for publication in *Acta Met.*